

Systematic study of the structure of odd-mass lanthanum nuclei. I. Levels in ^{137}La from $^{137}\text{Ce}^{m+g}$ decay*

E. A. Henry, N. Smith, P. G. Johnson, and R. A. Meyer

Lawrence Livermore Laboratory, Livermore, California 94550

(Received 31 March 1975)

The level structure of ^{137}La populated by the β decay of $^{137}\text{Ce}^{m+g}$ was studied by γ -ray and conversion-electron spectroscopy using mass-separated sources, large-volume and Compton-suppressed Ge(Li) detectors, and a Si(Li) detector. Nine previously unreported transitions were observed and two more levels were established in ^{137}La . The ^{137}La level structure is discussed in terms of the weak-coupling model.

[RADIOACTIVITY $^{137}\text{Ce}^{m+g}$ [from $^{136}\text{Ce}(n, \gamma)$ and $\text{Ba}(\alpha, Xn\gamma)$]; measured E_γ , I_γ , I_{ce} ; deduced $\log ft$. ^{137}La deduced ICC, levels, J , π . Mass separation, Ge(Li) and Si(Li) detectors, Compton suppression spectrometer.]

I. INTRODUCTION

A systematic study of the odd-mass lanthanum nuclei ($Z=57$) presents an opportunity to study the effects of several nuclear models. First, the lanthanum nuclei have seven protons outside the $Z=50$ closed shell. They provide a natural extension of the systematics of the antimony ($Z=51$),¹ iodine ($Z=53$),¹ and cesium ($Z=55$) nuclei. Secondly, the lanthanum nuclei that can be studied experimentally range from the neutron-deficient ^{125}La through the singly magic ^{139}La to the neutron-rich ^{147}La . The present studies concentrate on a region of rapid transition from nuclei that are soft towards deformation² to nuclei with nearly spherical shape.³ The nucleus ^{137}La is in the more vibrational class of nuclei. Therefore, for later comparison, it is important to understand the level structure and properties of ^{137}La in as much detail as possible.

In early studies of $^{137}\text{Ce}^{m+g}$ decay by Brosi and Ketelle⁴ and Dzhelepov *et al.*,⁵ two transitions with energies of 10 and 445 keV were observed and assigned to $^{137}\text{Ce}^g$ decay. The 10-keV transition was determined to be $M1$ from its conversion coefficient. Brosi and Ketelle proposed excited levels at 10 and 445 keV in ^{137}La . In 1963, Ruby, Hazoni, and Pasternak⁶ determined the half-life of the 10-keV level to be 89 ± 4 ns and confirmed the conversion coefficient measurement of Brosi and Ketelle.

Since 1963, only three studies of $^{137}\text{Ce}^{m+g}$ decay to levels in ^{137}La have been reported. In 1964, Frankel⁷ studied both γ rays and conversion electrons from $^{137}\text{Ce}^{m+g}$ decay and developed a level scheme for ^{137}La . Shortly thereafter, Van Hise, Chilosi, and Stone⁸ determined an upper limit for the half-life of the 1004-keV level in ^{137}La and discussed the $M2$ and $E3$ transitions depopulating it.

In 1969, Beery⁹ repeated the γ -ray studies of Frankel and obtained photon intensities which differed from those of Frankel by as much as a factor of 2 for weak transitions. No new transitions or levels were assigned to ^{137}La by Beery. Of these three studies, only the work of Van Hise *et al.* is published; the data of Frankel are compiled in the *Table of Isotopes*.¹⁰ The present experiment was undertaken to confirm the unpublished work of Frankel and Beery and to look for previously unobserved transitions and levels.

The $^{137}\text{Ce}^{m+g}$ sources for this experiment were made by both $^{136}\text{Ce}(n, \gamma)$ and $^{134}\text{Ba}(\alpha, Xn)$. Sources made by the latter method were mass separated. The $^{137}\text{Ce}^{m+g}$ decay was studied by both γ -ray and conversion-electron spectroscopy. Although the ^{137}La level scheme was thought to be well known, nine previously unreported transitions were observed in this study, and two more levels were established.

Section II describes the experimental procedures used in this work. The data results are presented in Sec. III. Spin and parity assignments to the ^{137}La levels are also outlined in this section. In Sec. IV, some aspects of the ^{137}La nuclear structure are discussed, including an interpretation of the levels in terms of the weak-coupling model.

II. EXPERIMENTAL PROCEDURE

Sources of radioactive $^{137}\text{Ce}^{m+g}$ were prepared for study by neutron capture and by the (α, Xn) reaction on enriched ^{134}Ba . The neutron capture sources were made by irradiating enriched ^{136}Ce at the Livermore pool type reactor. This source was counted directly with no chemistry or mass separation. Other sources, made by α bombardment of barium at the 88-inch cyclotron at Lawrence Berkeley Laboratory, were transported to

Lawrence Livermore Laboratory where the cerium was chemically separated from the target material and then mass separated. The chemical techniques used were those described in Appendix A for separation of Ce activity from BaCO_3 target material.

γ -ray spectroscopy was performed on the neutron capture source using a Compton-suppressed Ge(Li) detector and a large-volume (about 40 cm^3) Ge(Li) detector. Energy calibration was facilitated by small amounts of $^{139,140,142}\text{Ce}$ in the ^{136}Ce sample, as well as minute amounts of ^{55}Mn , ^{151}Eu , and ^{164}Dy contaminants which have large capture cross sections. Thus γ rays following the decay of $^{139,141,143}\text{Ce}$, ^{56}Mn , ^{152}Eu , and ^{165}Dy served as calibration lines. The decay of this neutron capture source was followed for six days and γ -ray half-lives were obtained.

Mass-separated sources deposited on an aluminum foil were used for both γ -ray and conversion-electron spectroscopy. A 0.7-cm^3 planar, low-energy photon spectrometer (LEPS) was employed in an attempt to observe the 10.56-keV γ ray. This γ ray was easily observed, though the detector was not well enough calibrated at this low energy for reliable energy or intensity determination. The 87.2-keV γ ray was also observed using the LEPS. Because of Pb x-ray interference, this γ ray was not observed with other detectors. Conversion-electron data were taken using a 4-mm -thick Si(Li) detector and useful conversion-electron intensities were obtained for 11 transitions.

Both the γ -ray and conversion-electron spectra were analyzed using the computer code GAMANAL,¹¹ which determined both energies and intensities. The peak shape parameters used by GAMANAL were suitably adjusted in order to analyze the conversion-electron data.

III. DATA AND RESULTS

The transitions which follow ^{137}Ce decay are divided into two groups: those which follow $^{137}\text{Ce}^e$ decay and those which follow $^{137}\text{Ce}^m$ decay. The 10.56-keV transition is the only one common to each decay. Assignment was easily made on the basis of source preparation, mass separation, and half-life. Feeding of the ground state of ^{137}Ce by the very intense isomeric transition in ^{137}Ce caused the transitions which follow $^{137}\text{Ce}^e$ decay to have a characteristic two-component decay.

Figure 1 shows two portions of a γ -ray singles spectrum from $^{137}\text{Ce}^{m+g}$ obtained with a large-volume Ge(Li) detector. The ^{137}Ce source for this spectrum was mass-separated. Clearly present in the lower energy portion are the previously unreported 906.84-keV and 917.45-keV γ rays. In the higher energy portion are seen the $E3$ 993.81-keV

γ ray and the predominately $M2$ 1004.49-keV γ ray.

Nineteen γ rays were assigned to $^{137}\text{Ce}^e$ decay and are summarized in Table I. These transitions are normalized to $I_\gamma(\text{rel.})=1000$ for the 447.15-keV transition. Eleven γ rays were assigned to $^{137}\text{Ce}^m$ decay, including the 10.56-keV transition and the 254.29-keV isomeric transition. Normalization for these γ rays is made to $I_\gamma(\text{rel.})=1000$ for the 824.82-keV transition. Data for these γ rays are summarized in Table II.

The conversion-electron data for $^{137}\text{Ce}^e$ and $^{137}\text{Ce}^m$ decays are summarized in Tables III and IV, respectively. Because the 254.29-keV conversion-line intensity was over three orders of magnitude greater than the intensity of the 447.15-keV conversion lines, the isomeric transition dominated the spectrum and severely limited the statistics of other conversion lines. Nevertheless, useful information could be extracted from the conversion-electron spectrum. The conversion line intensities for transitions following $^{137}\text{Ce}^e$ decay are normalized to $I_k(\text{rel.})=100$ for the 447.15-keV transition. Normalization is made to $I_k(\text{rel.})=1$ for the 824.82-keV transition for conversion electron lines following $^{137}\text{Ce}^m$ decay.

Conversion coefficients for transitions following $^{137}\text{Ce}^e$ decay were determined from the γ -ray and conversion-electron intensities by requiring $\alpha_k = 0.0136 \pm 0.0014$ for the 447.15-keV transition. This conversion coefficient was obtained by assuming $\alpha_k = 5.54$ for the $M4$ isomeric transition, and by using the 447.15-keV to 254.29-keV γ -ray and conversion-electron ratios from spectra in which the $^{137}\text{Ce}^m$ and $^{137}\text{Ce}^e$ decays were in transient equilibrium.

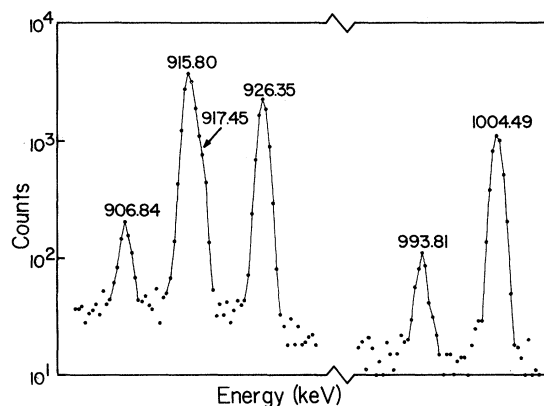


FIG. 1. Two portions of the γ -ray singles spectrum from a mass-separated $^{137}\text{Ce}^{m+g}$ source. Included are the previously unreported 906.84-keV and 917.45-keV γ rays, the $E3$ 993.81-keV γ ray, and the predominately $M2$ 1004.49-keV γ ray.

TABLE I. γ rays which follow $^{137}\text{Ce}^g$ decay.

E_γ	I_γ (rel.) ^a	Assignment from-to
10.56 (4) ^{b,c}		10-0
148.83 (8)	0.5 (2)	641-493
217.03 (5)	2.2 (3)	926-709
433.22 (9)	29.1 (15)	926-493
436.59 (9)	149 (5)	447-10
447.15 (8)	1000 ^d	447-0
479.12(10)	6.7 (3)	926-447
482.47(10)	25.7 (9)	493-10
493.03(10)	5.9 (3)	493-0
529.3 (2)?	0.2 (1)	(1171-641)
631.38 (6)	7.5 (4)	641-10
678.26(12)	0.5 (2)	1171-493
698.72(11)	17.5 (9)	709-10
709.72(11)	0.6 (1)	709-0
724.4 (3)	0.4 (2)	1171-447
770.97(10)	3.4 (2)	781-10
781.57(13)	1.7 (2)	781-0
915.80(13)	28.9 (10)	926-10
926.35(13)	19.0 (7)	926-0
1160.85(22)	0.84 (8)	1171-0

^a To obtain absolute photon intensities, multiply by 0.00224(10).

^b 10.56 keV obtained from energy differences of cascade and crossover transitions, $E_\gamma = 10.61$ keV using a LEPS; see text.

^c Uncertainties in the last significant figures are shown in parentheses.

^d In transient equilibrium spectra $I(254\gamma)/I(447\gamma) = 4.91(15)$.

Normalization for the conversion coefficients following $^{137}\text{Ce}^m$ decay was made to the theoretical $E2$ conversion coefficient for the 824.82-keV transition, $\alpha_k = 0.00250$. As discussed below, the 824.82-keV transition is shown to be an $E2$ transition. Additionally, since $\alpha_k = 5.54$ for the $M4$ isomeric transition, $\alpha_k = 0.00247 \pm 0.00019$ from experiment for the 824.82-keV transition, consistent with an $E2$ multipolarity. For the 254.29-keV $M4$ isomeric transition, $K/L = 2.84$ from theory¹² while $K/L = 2.80 \pm 0.22$ was obtained in this experiment.

The transition multiplicities indicated in Tables III and IV are proposed by comparing the deduced experimental conversion coefficients with the theoretical values of Hager and Seltzer.¹² In addition to the multiplicities determined here, Frankel showed that the 169.26-keV transition has an $E1$ multiplicity.

Decay schemes for $^{137}\text{Ce}^g$ and $^{137}\text{Ce}^m$ were constructed using γ -ray energy sums. In addition, the coincidence results of Frankel show that the 169.26-keV γ ray is in coincidence with the 835.29-

TABLE II. γ rays which follow $^{137}\text{Ce}^m$ decay.

E_γ	I_γ (rel.) ^a	Assignment from-to
10.56 (4) ^{b,c}		10-0
87.2 (2)	20(3)	1004-926
169.26 (4)	995(60)	1004-835
254.29 (5) ^d	24 800(900)	$^{137}\text{Ce}^m$ - $^{137}\text{Ce}^g$
762.30(10)	435(20)	762-0
824.82(12)	1000	835-10
835.38(12)	234(10)	835-0
906.84(16)	6.3(11)	917-10
917.45(17)	29(5)	917-0
993.81(21)	4.5(6)	1004-10
1004.49(20)	51(6)	1004-0

^a To obtain absolute photon intensities, multiply by 0.000441(20).

^b See Table I.

^c Uncertainties in the last significant figures are shown in parentheses.

^d Isomeric transition.

and 842.74-keV γ -ray pair and the 479.12-keV γ ray is in coincidence with the 447.15-keV γ ray. Frankel also observed that when a coincidence gate was set mainly on the 915.80- and 926.35-keV γ rays using a NaI gating detector, a peak at 85 keV appeared. Such a result is consistent with the establishment of the 917.42-keV level in this work and the fact that this level is populated by the 87.2-keV transition and depopulated by the 917.45- and 906.84-keV transitions.

The decay schemes for $^{137}\text{Ce}^g$ and $^{137}\text{Ce}^m$ are shown in Figs. 2 and 3. The absolute transition intensities were obtained by requiring a total of

TABLE III. Conversion electron data for transitions which follow $^{137}\text{Ce}^g$ decay.

Conversion line	I_{ce} (rel.)	α^a	Λ
433K	2.6 (9) ^b	0.013 (5)	$E2$
436K	12.6 (15)	0.012 (2)	$E2$
L	2.2 (8)	0.0020 (8)	
447K	100 (5)	0.0136(14)	$M1 + E2$
L	12.8 (16)	0.0017 (4)	
M	2.9 (9)	0.00040(13)	
698K	0.63 (9)	0.0050(10)	$M1(+E2)$
916K	0.53 (9)	0.0025 (5)	$(M1 + E2)$
926K	0.29 (3)	0.0023 (4)	$(M1 + E2)$

^a Normalized to $\alpha_k(447\gamma) = 0.0136(14)$; this conversion coefficient is obtained assuming $\alpha_k(254\gamma) = 5.54$, and using γ -ray and conversion-electron intensity ratios from spectra in which the $^{137}\text{Ce}^m$ decays are in transient equilibrium.

^b Uncertainties in the last significant figures are shown in parentheses.

TABLE IV. Conversion-electron data for transitions following $^{137}\text{Ce}^m$ decay.

Conversion line	I_{ce} (rel.)	α^a	Λ
254K	55 500(3300) ^b	5.54 ^c	M4
L	19 800(1000)	1.98 (1)	
MN...	6000(400)	0.60 (4)	
762K	0.51 (3)	0.0030(3)	E2
L	0.069(16)	0.0004(1)	
824K	1.00 (3)	0.002 50 ^d	E2
L	0.127(12)	0.000 31(4)	
835K	0.208(16)	0.0022(3)	E2
1004K	0.114(13)	0.0056(9)	M2(+E3)

^a Normalized to $\alpha_k(824\gamma) = 0.002 50$.

^b Uncertainties in the last significant figures are shown in parentheses.

^c Theoretical α_k for an M4 transition.

^d α_k for a pure E2 transition; the experimental value is $\alpha_k(824\gamma) = 0.002 47(19)$ if $\alpha_k(254\gamma) = 5.54$.

100 γ -ray, conversion-electron, and electron-capture transitions out of the $^{137}\text{Ce}^m$ decay scheme. The $\epsilon + \beta^+$ intensity of the first forbidden unique transition to the ^{137}La ground state is assumed to be negligible. The absolute transition intensities for the $^{137}\text{Ce}^e$ decay scheme were determined by requiring that, during transient equilibrium, the total $^{137}\text{Ce}^e$ β -decay intensity equals the total intensity of the 254.29-keV isomeric transition. The decay branches to the levels in each decay scheme are deduced by requiring an intensity balance at each level. $\log ft$ values are calculated assuming a Q_ϵ value of 1240_{-30}^{+20} keV for decay of $^{137}\text{Ce}^e$. The decay branches and $\log ft$ values are summarized in Table V.

The Q_ϵ value of 1240_{-30}^{+20} keV was obtained by

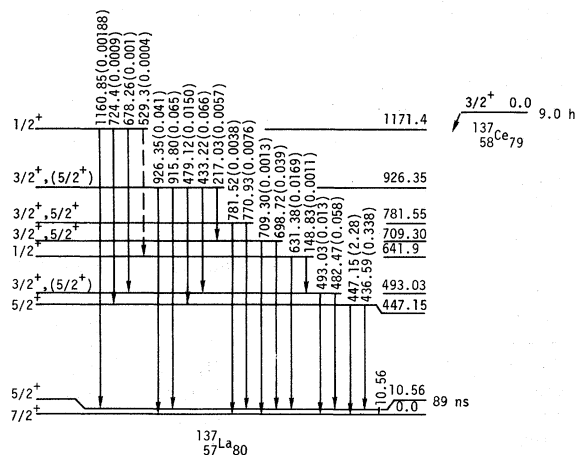


FIG. 2. The ^{137}La level scheme resulting from the decay of $^{137}\text{Ce}^e$.

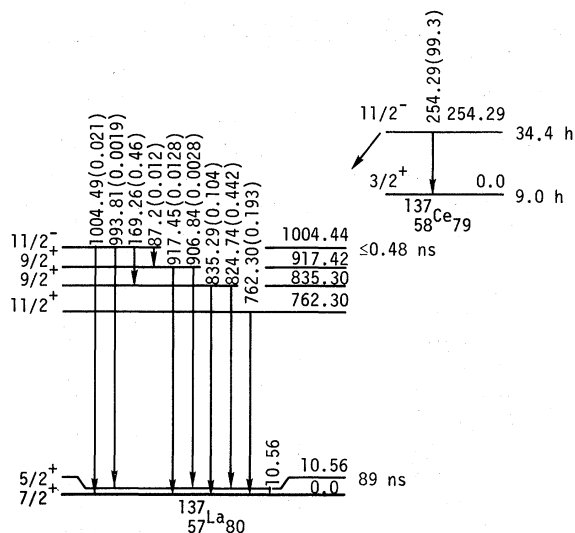


FIG. 3. The ^{137}La level scheme resulting from the decay of $^{137}\text{Ce}^m$. Also shown is the isomeric decay in ^{137}Ce .

comparing the experimental and theoretical values of ϵ/β^+ for decay to the 10.56-keV level. Experimentally, the positron intensity (I_{β^+}) was determined by comparing one-half of the annihilation radiation intensity [$I(511 \text{ peak}) = 14 \pm 2$ relative units] obtained using a mass-separated sample with total 254.29-keV isomeric transition intensity in an equilibrium spectrum. Taking into consideration the possible annihilation radiation resulting from $^{137}\text{Ce}^m$ β decay to the ^{137}La ground state, $I_{\beta^+} = (0.0136_{-0.0040}^{+0.0020})\%$. Q_ϵ was then determined by comparing the experimental value of $\log(f_0^\epsilon/f_0^+)$ = $3.85_{-0.07}^{+0.15}$ with the calculations of Gove and Mar-

TABLE V. β -decay branches and $\log ft$ values from $^{137}\text{Ce}^e$ decay (G) and $^{137}\text{Ce}^m$ decay (M).

Level	Populated by	I_ϵ (%)	$\log ft$
10.56	G	97.14 (13) ^{a,b}	5.4
447.15	G	2.60 (12)	6.6
493.03	G	0.0028(66)	≥ 8.9
641.9	G	0.0180(15)	8.5
709.30	G	0.035 (4)	8.1
762.30	M	0.193 (13)	8.2
781.55	G	0.0114 (9)	8.4
835.30	M	0.09 (5)	$8.4_{-0.2}^{+0.4}$
917.4	M	0.0036(32)	≥ 9.4
926.35	G	0.193 (8)	6.8
1004.55	M	0.49 (4)	7.4
1171.4	G	0.0043 (9)	$6.7_{-0.5}^{+1.7}$

^a Includes the positron decay intensity of $(0.0136_{-0.0040}^{+0.0020})\%$.

^b Uncertainties in the last significant figures are given in parentheses.

tin.¹³ The resulting Q_ϵ value agrees with the value of $Q_\epsilon = 1200 \pm 30$ keV quoted in the 1971 Atomic Mass Evaluation.¹⁴

Spin and parity assignments to levels in ^{137}La are made on the basis of the $\log ft$ values, γ -ray branching, transition multipolarity, systematics, and for some levels by appeal to the weak-coupling model. These spin and parity assignments are summarized in the following four paragraphs.

The ground state spin of ^{137}La has been determined to be $\frac{7}{2}$ from hyperfine structure in an optical spectroscopy experiment.¹⁵ There are no experimental data on which to definitely establish the parity as positive; however, it is consistent with systematics and the very long half-life for β decay to the $\frac{3}{2}^+$ ^{137}Ba ground state. The first excited level at 10.56 keV decays by an $M1$ transition to the ^{137}La ground state. Since this level is populated by allowed β decay from the known $J = \frac{3}{2}$ ^{137}Ce ground state, the 10.56-keV level has $J^\pi = \frac{5}{2}^+$ and the ^{137}Ce ground state has positive parity.

Of the seven other excited levels populated by $^{137}\text{Ce}^\beta$ decay, five have transitions to both the ground state and the 10.56-keV level. Four of these levels at 447.15, 709.30, 781.55, and 926.35 keV are populated by allowed or first forbidden β decay. Since all are below the $\frac{4}{2}^+$ level and no other negative parity levels are expected below the $\frac{11}{2}^-$ level in ^{137}La , these four levels have $J^\pi = \frac{3}{2}^+$ or $\frac{5}{2}^+$. Further, the $M1 + E2$ multipolarity of the 447.15-keV transition limits J^π to $\frac{5}{2}^+$ for the 447.15-keV level. Because this level is one of three with $\log ft$ values between 6 and 7 while most $\log ft$ values are greater than 8, a small mixing of the $2d_{5/2}$ single-particle orbital in its wave function may be indicated. Similarly, the $\log ft$ value of 6.8 for the 926.35-keV level may indicate a contribution from the $2d_{3/2}$ single-particle orbital in its wave function. Thus, the spin and parity of the 926.35-keV level is suggested to be $\frac{3}{2}^+$ although $\frac{5}{2}^+$ cannot be ruled out on experimental grounds. The γ -ray population and depopulation of the 493.03-keV level is similar to that of the above four levels, suggesting $J^\pi = \frac{3}{2}^+$ or $\frac{5}{2}^+$. The systematics of the odd-mass lanthanum nuclei favors a $\frac{3}{2}^+$ assignment for the 493.03-keV level.

The two levels at 641.9 and 1171.4 keV do not have depopulating transitions to the $\frac{7}{2}^+$ ground state, but do have transitions to $\frac{5}{2}^+$ and $\frac{3}{2}^+$ levels. Thus $J^\pi = \frac{1}{2}^+$ is indicated for these two levels.

In addition to the 10.56-keV level populated through γ -ray transitions, four other excited levels are populated by $^{137}\text{Ce}^m$ decay. The 1004.44-keV level is identified in the $^{136}\text{Ba}(\alpha, t)$ reaction studies of Nakai *et al.*¹⁶ as the $h_{11/12}$ single-particle level. The K conversion coefficient of the 1004.49-keV transition is consistent with an $M2$ multipolar-

ity. The $\log ft$ value for decay to the 835.30-keV level, the $E1$ 169.26-keV transition from the $\frac{11}{2}^-$ 1004.44-keV level, and the decay of the level to the 10.56-keV level and the ground state limit J^π to $\frac{9}{2}^+$ for the 835.30-keV level. Thus the 824.74-keV transition has an $E2$ multipolarity, consistent with the experimentally determined K conversion coefficient. The 917.42-keV level is also proposed to be $\frac{9}{2}^+$. The 87.2-keV transition populating this level can only be $E1$ or $E1 + M2$. For any other multipolarity, the total intensity of the 87.2-keV transition would substantially exceed the total intensity depopulating the 917.42-keV level. Finally, a 762.30-keV transition with $E2$ multipolarity is observed which is assigned to $^{137}\text{Ce}^m$ decay. No other transitions are observed which determine the placement of the 762.30-keV transition on the basis of energy sums. Thus a level at 762.30 keV with $J^\pi = \frac{11}{2}^+$ is proposed which has a transition only to the $\frac{7}{2}^+$ ground state.

Comparing this study with the works of Frankel⁷ and Beery⁹ shows that two new levels at 641.9 and 917.42 keV are established. Also, Frankel suggested that the 709-keV level had $J^\pi = \frac{1}{2}^+$; however, in the present study the observation of a transition to the $\frac{7}{2}^+$ ^{137}La ground state rules out this possibility. Instead, we propose that the 641.9-keV level has $J^\pi = \frac{1}{2}^+$, since no ground state transition is observed for that level. The 1171.4-keV level is well established by three depopulating transitions in this work. (In the compilation of Frankel's data in the *Table of Isotopes*, this level is erroneously indicated at 1160 keV.) In general, the transition intensities obtained in this study are in better agreement with those of Beery than with those of Frankel.

IV. DISCUSSION

Because of its nearness to the singly magic ^{139}La nucleus, ^{137}La is expected to be a spherical nucleus which can be described by weak coupling of the odd proton to a vibrating core.¹⁷ Comparing the predictions of such a model with the experimental results for ^{137}La requires some care, because the assumption of this model was implicit in the spin and parity assignments to several of the ^{137}La excited levels. Nevertheless, the qualitative agreement between the experimental levels and predictions of the weak-coupling model is good.

The single-particle levels available to the odd proton in ^{137}La are the $1g_{7/2}$, $2d_{5/2}$, $2d_{3/2}$, $3s_{1/2}$, and $1h_{11/2}$ single-particle orbitals. The lowest core excitation in ^{136}Ba is the 2^+ level at 818.50 keV.¹⁸ The next excited level in the ^{136}Ba core is at 1551.0 keV and would not be expected to make any substantial contribution when considering the low-

lying level structure of ^{137}La . By considering the above single-particle levels and the coupling of the $1g_{7/2}$ and $2d_{5/2}$ single-particle levels to the 2_1^+ core excitation in ^{136}Ba , all of the proposed levels in ^{137}La can be accounted for. Only two $\frac{7}{2}^+$ levels predicted by the weak-coupling model are not seen in ^{137}La . This is not unexpected, since direct β decay to these levels would require $\Delta J=2$ from either $^{137}\text{Ce}^e$ or $^{137}\text{Ce}^m$. Also, population of the $\frac{7}{2}^+$ levels by γ -ray cascade would be unlikely since these levels would probably lie in the region between 600 and 1000 keV, where competing $E2$ transitions to lower excited levels would dominate.

The $\frac{7}{2}^+$ ground state and $\frac{9}{2}^+$ 10.56-keV level are largely $1g_{7/2}$ and $2d_{5/2}$ single-particle states. The assignment of these configurations are supported by the (α, t) reaction studies of Nakai *et al.*¹⁶ The coupling of these two single-particle states to the 2_1^+ core state account for the $\frac{11}{2}^+$ and two $\frac{9}{2}^+$ levels populated in $^{137}\text{Ce}^m$ decay. The $\frac{11}{2}^+$ level has the configuration $1g_{7/2} \otimes 2_1^+$ using weak coupling, while the $\frac{9}{2}^+$ levels are mixtures of the $2d_{5/2} \otimes 2_1^+$ and $1g_{7/2} \otimes 2_1^+$ configurations. Assuming that there are no contributions from other configurations to the $\frac{9}{2}^+$ levels, that the ground state and the 10.56-keV level are pure single-particle states, and that only pure $E2$ transitions occur, we can determine the wave functions of the $\frac{9}{2}^+$ levels from the branching ratios:

835-keV level:

$$(0.82)^{1/2}(2d_{5/2} \otimes 2_1^+)_{9/2} + (0.18)^{1/2}(1g_{7/2} \otimes 2_1^+)_{9/2}$$

917-keV level:

$$(0.18)^{1/2}(2d_{5/2} \otimes 2_1^+)_{9/2} + (0.82)^{1/2}(1g_{7/2} \otimes 2_1^+)_{9/2}$$

A detailed comparison of levels with a spin of $\frac{3}{2}$ or $\frac{5}{2}$ with the predictions of the weak-coupling is not possible because of uncertainties in the assigned spins. However, as indicated earlier, the experimental levels which could have $J^\pi = \frac{3}{2}^+$ or $\frac{5}{2}^+$ can be accommodated qualitatively within the weak-coupling model when the $2d_{3/2}$ single-particle orbital is included. Two $\frac{1}{2}^+$ levels are expected at approximately 1 MeV: one having the $3s_{1/2}$ single-particle configuration and the other, the $2d_{5/2} \otimes 2_1^+$ configuration. Levels observed at 1171.4 and 641.9 keV have $J^\pi = \frac{1}{2}^+$. The 1171.4-keV level may have larger contribution from the $3s_{1/2}$ orbital than the 641.9-keV level on the basis of its lower, but uncertain, $\log ft$ value.

The 1004.44-keV level has been shown to be largely the $h_{11/2}$ single-particle level by Nakai *et al.*¹⁶ Van Hise *et al.*⁸ determined an upper limit for the half-life of this level of 0.41 ± 0.07 ns. Assuming that the half-life of the 1004.44-keV level is ≤ 0.48 ns, the hindrance factors relative

to the Weisskopf estimate for the transitions depopulating this level are calculated and summarized in Table VI. From the K conversion coefficient, the multipolarity of the 1004.49-keV transition is $M2 + (5^{+39})\% E3$, and both the $M2$ and $E3$ hindrances for this transition are determined. The $E3$ enhancements of the 993.81- and 1004.49-keV transitions are ≥ 9.1 and ≥ 4.6 , respectively, indicating some contribution from the $1g_{7/2} \otimes 3_1^-$ and $2d_{5/2} \otimes 3_1^-$ configurations to the 1004.44-keV level as suggested by Van Hise *et al.* Here the 3_1^- state is the octopole vibration. The 169.26- and 87.2-keV $E1$ transitions are hindered by factors of $\leq 1.03 \times 10^4$ and $\leq 7.0 \times 10^4$, respectively. Such hindrances are in line with the systematics of $E1$ transitions from $\frac{11}{2}^-$ levels to predominantly phonon-coupled levels.¹

Thus we see that the low-lying level structure of ^{137}La can be qualitatively accounted for by a weak-coupling model. The characteristics of the wave functions of two of the core multiplet levels have been quantified by making appropriate assumptions concerning mixing from higher lying core states and transition multipolarities. In later papers in this series, the level structure of ^{137}La will be compared to the systematics of other odd-mass lanthanum nuclei.

The authors express their appreciation to the crews of the Livermore pool type reactor and 88-in. cyclotron at Lawrence Berkeley Laboratory for irradiating the targets.

APPENDIX

During this systematic study of odd-mass lanthanum level structure from the β decay of cerium, chemistry techniques were necessary to extract the cerium activity from the barium target material and to prepare it for mass separation. For studies in which the lanthanum daughter activity interfered significantly, further chemistry was performed to remove the cerium plus lanthanum activity from aluminum foils and provide a cer-

TABLE VI. Hindrance factors for transitions depopulating the 1004.44-keV level, assuming $T_{1/2}$ (level ≤ 0.48 ns).

E_γ	Λ	Hindrance ^a
87.2	$E1$	$\leq 7.0 \times 10^4$
169.26	$E1$	$\leq 1.03 \times 10^4$
993.81	$E3$	≤ 0.11
1004.49	$M2^b$	≤ 10.6
	$E3^b$	≤ 0.22

^a The ratio of the γ -ray partial half-life and the Weisskopf estimate of the half-life, $T_{\gamma_{1/2}}(\text{exp})/T_{1/2}(\text{WE})$.

^b Assuming $\Lambda = 95\% M2 + 5\% E3$; see text.

ium-lanthanum separation. These chemistry techniques are described briefly in this Appendix.

The BaCO₃ target with the Ce products was dissolved in warm 6 M (HCl) containing 200 μg of Ce⁺³ carrier. A Ce-Ba separation was done by twice precipitating Ce with NH₄OH and centrifuging off the barium containing supernatant liquid. The remaining Ce(OH)₃ precipitate was dissolved in 6 M HCl, and cerium oxalate precipitated after adjusting the pH to approximately 5 with NH₄OH. The H₂O-washed and dried precipitate was ignited at 850°C, then transferred to a tungsten mass-separator crucible.

After mass separation, Ce samples (on Al foils) were separately dissolved in 6 M HCl containing

3 mg each Ce⁺³ and La⁺³ carriers, plus a few μ of concentrated HNO₃. An aluminum leach was done by twice precipitating Ce and La with 25% NaOH and discarding the Al-containing liquid. After dissolving the hydroxide precipitates in concentrated HNO₃, a Ce-La separation was done by twice oxidizing Ce with NaBrO₃ and precipitating Ce as cerium iodate. The cerium iodate from each sample was filtered onto a small filter for counting.

The La fraction from each sample was further purified by one more Ce iodate precipitation. La fluoride and La oxalate precipitations completed the purification. The La fraction was separated into several portions for counting.

*Work performed under the auspices of the U. S. Energy Research and Development Administration.

¹R. A. Meyer, in Proceedings of the IUPAP Conference on Gamma Ray Transition Probabilities, Delhi, India, 1974 (unpublished).

²E. A. Henry and R. A. Meyer, *Z. Phys.* **271**, 75 (1974).

³E. A. Henry and R. A. Meyer, following paper, *Phys. Rev. C* **12**, 1321 (1975).

⁴A. R. Brosi and B. H. Ketelle, *Phys. Rev.* **103**, 917 (1956).

⁵B. S. Dzhelepov, B. K. Preobrazhenskii, I. M. Rogachev, and P. A. Tishkin, *Izv. Akad. Nauk SSSR Ser. Fiz.* **22**, 931 (1958) [*Bull. Acad. Sci. USSR* **22**, 923 (1958)].

⁶S. L. Ruby, Y. Hazoni, and M. Pasternak, *Phys. Rev.* **129**, 826 (1963).

⁷R. B. Frankel, Ph.D. thesis, University of California, 1964 (unpublished).

⁸J. R. Van Hise, G. Chilosi, and N. J. Stone, *Phys. Rev.* **161**, 1254 (1967).

⁹D. B. Beery, Ph.D. thesis, Michigan State University, 1969 (unpublished).

¹⁰C. M. Lederer, J. M. Hollander, and I. Perlman, *Table of Isotopes* (Wiley, New York, 1967), 6th ed.

¹¹R. Gunnick and J. B. Niday, Lawrence Livermore Laboratory, Report No. UCRL-51061, 1971, 1972 (unpublished), Vols. I-IV.

¹²R. S. Hager and E. C. Seltzer, *Nucl. Data* **A4**, 1 (1968).

¹³N. B. Gove and M. J. Martin, *Nucl. Data* **A10**, 206 (1971).

¹⁴A. H. Wapstra and N. B. Gove, *Nucl. Data* **A9**, 265 (1971).

¹⁵W. Fischer, H. Hühnermann, and K. Mandrek, *Z. Phys.* **254**, 127 (1972).

¹⁶K. Nakai, P. Kleinheinz, J. R. Leigh, K. H. Maier, F. S. Stephens, R. M. Diamond, and G. Løvghøiden, *Phys. Lett.* **44B**, 443 (1973).

¹⁷A. de-Shalit, *Phys. Rev.* **122**, 1530 (1961).

¹⁸See for example R. A. Meyer and R. G. Griffioen, *Phys. Rev.* **186**, 1221 (1969).